

Experimental Test of the Inter-Layer Pairing Models for High- T_c Superconductivity Using Grazing Incidence Infrared Reflectometry.

J. Schützmann,¹ H. S. Somal,¹ A. A. Tsvetkov,^{1,2} D. van der Marel,¹ G. E. J. Koops,¹ N. Kolesnikov,³ Z. F. Ren,⁴ J.H. Wang,⁴ E. Brück,⁵ and A. A. Menovsky⁵

¹ *Materials Science Centre, Laboratory of Solid State Physics, University of Groningen, Nijenborgh 4, 9747 AG Groningen, The Netherlands.*

² *P.N. Lebedev Physical Institute, Russian Academy of Sciences, Moscow, 117924 Russia*

³ *Inst. of Solid State Physics, Russian Academy of Sciences, Chernogolovka, 142432 Russia*

⁴ *Dept. of Chemistry, Suny at Buffalo, Buffalo NY 14260-3000, USA*

⁵ *Van der Waals-Zeeman Institute, University of Amsterdam, The Netherlands.*

(19 august 1996, Phys. Rev. B, to be published in 1997)

From measurements of the far-infrared reflectivity at grazing angles of incidence with p-polarized light we determined the c-axis Josephson plasma frequencies of the single layer high T_c cuprates $Tl_2Ba_2CuO_6$ and $La_{2-x}Sr_xCuO_4$. We detected a strong plasma resonance at 50 cm^{-1} for $La_{2-x}Sr_xCuO_4$ in excellent agreement with previously published results. For $Tl_2Ba_2CuO_6$ we were able to determine an upper limit of the unscreened c-axis Josephson plasma frequency 100 cm^{-1} or a c-axis penetration depth $> 15\mu\text{m}$. The small value of ω_J stands in contrast to recent a prediction based on the inter-layer tunneling mechanism of superconductivity.

PACS: 74.25.Gz, 78.30.Er, 71.45.Gm, 74.25.Nf

A striking feature of the high T_c cuprates is the strong anisotropy of the conductivity. Both the low conductivity in the c-direction (below the Mott limit) and the frequency dependence (no Drude peak) support the 'confinement' hypothesis [1] stating that hopping of single electrons between neighboring CuO_2 planes is inhibited in the normal state due to spin-charge separation. As tunneling of pairs of carriers is still allowed, the formation of Cooper-pairs results in a gain of kinetic energy, which stabilizes the superconducting state. Therefore within the Chakravarty-Anderson interlayer model the main contribution to the condensation energy (E_{cond}) is due to the Josephson coupling between adjacent CuO_2 planes. Recently Anderson [2] pointed out that, since the Josephson coupling energy is proportional to the plasma frequency of the condensate (ω_J), a proportionality should exist between ω_J and T_c for the cuprates with one CuO_2 layer per unit cell. One of the best compounds for testing the confinement hypothesis appears to be $Tl_2Ba_2CuO_y$ at optimal oxygen concentration due to its high value of T_c (85 K) and the large separation between CuO_2 planes (11.57Å). According to the ILT hypothesis [2-4]:

$$\hbar^2\omega_J^2 = \eta E_{cond} \frac{16\pi d e^2}{a^2} \quad (1)$$

where η represents the fraction of the condensation energy contributed by the ILT mechanism [4], d is the spacing between adjacent CuO_2 -planes and a is the in-plane lattice parameter. The condensation energy ($E_{cond} \propto T_c^2$) can be obtained directly from the specific heat [5], resulting in $E_{cond} = 80\mu\text{eV}$ per unit of CuO_2 for $Tl_2Ba_2CuO_y$ ($T_c=85\text{ K}$) and $13\mu\text{eV}$ for slightly un-

derdoped $La_{2-x}Sr_xCuO_4$ ($T_c=32\text{ K}$). The above expression for ω_J is radically different from conventional BCS-theory, where, adopting a 'dirty-limit' scenario for the c-axis conductivity, ω_J^2 follows from the Glover-Tinkham-Ferrel sumrule [6]

$$\hbar^2\omega_J^2 = 4\pi^2\hbar\sigma_n\Delta(0) \quad (2)$$

Using the ILT prediction (Eq.1) we calculate that $\omega_J \approx 1500\text{cm}^{-1}$ for $Tl_2Ba_2CuO_y$ and 530 cm^{-1} for $La_{2-x}Sr_xCuO_4$ ($T_c=32\text{ K}$). In contrast, using Eq.2 we calculate $\omega_J \approx 200\text{ cm}^{-1}$ and 230 cm^{-1} for $Tl_2Ba_2CuO_y$ and $La_{2-x}Sr_xCuO_4$ respectively. These values for ω_J should still be complemented with the atomic polarizabilities and optical-phonon parameters for each of these compounds to obtain the full c-axis dielectric function

$$\epsilon_c = \epsilon_\infty - \frac{\omega_J^2}{\omega^2} + \frac{4\pi i}{\omega} \sigma_e + \sum_j \frac{S_j \omega_j^2}{\omega_j^2 - \omega(\omega + i/\tau_j)} \quad (3)$$

from which follows the position of the screened Josephson plasma-resonance.

Most experimental techniques aimed at measuring the c-axis penetration depth or ω_J require single crystals of sufficient thickness (several mm) in the c-direction. Lacking large crystals of $Tl_2Ba_2CuO_6$ we adopted a different approach: By measuring the intensities of p-polarized light reflected from the ab-surface at a grazing angle of incidence (80°) we can probe the longitudinal optical modes for the electric field vector along the c-axis including the c-axis Josephson plasmon. In this study we used several flux-grown $Tl_2Ba_2CuO_6$ single crystals from the same batch [7]. The typical size of the crystals is $2 \times 2\text{ mm}$ in the ab-plane and 0.1 mm along the c-direction. The

field-cooled and zero-field cooled DC magnetic susceptibility (inset of Fig. 1) shows a 10 K wide transition with an onset at 90 K. For the DC transport measurements four gold contacts were evaporated, followed by a mild baking at 250 °C. The arrangement of the four voltage and current contacts was selected for obtaining an accurate value of ρ_c , but only relative changes of ρ_{ab} could be obtained. Both ρ_c and ρ_{ab} have a linear temperature dependence (Fig. 1) as has been reported before for this compound by a number of groups [8]. The drop in resistivity takes place between 95 and 85 K. Details about the preparation and characterization of the $\text{Ti}_2\text{Ba}_2\text{CuO}_6$ films ($T_c = 80$ K) and of the $\text{La}_{2-x}\text{Sr}_x\text{CuO}_4$ crystals were described in Refs. [9] and [10] respectively.

For a strongly anisotropic material with a high conductivity in the ab-plane and a low conductivity along the c-axis, minima are found in the reflectivity

$$R_p = \left| \frac{Z_0 - Z_s^p}{Z_0 + Z_s^p} \right|^2 \quad (4)$$

when $\text{Re}Z_s^p$ has a maximum. Here Z_0 is the vacuum impedance. The surface impedance for p-polarized light at oblique incidence is

$$Z_s^p = \frac{Z_0}{n_{ab} \cos \theta} \sqrt{1 - \frac{\sin^2 \theta}{\epsilon_c}} \quad (5)$$

where θ is the angle of incidence with the surface normal, and $n_{ab}^2 = \epsilon_{ab}$ the ab-plane component of the dielectric tensor. The c-axis longitudinal modes appear as sharp resonances in the surface resistance [11], which is proportional to the pseudo-loss function

$$L(\omega) = \text{Im} e^{i\phi} \frac{\sqrt{1 - \frac{\sin^2 \theta}{\epsilon_c}}}{1 + |Z_s^p/Z_0|^2} = \frac{(1 - R_p)|n_{ab}| \cos \theta}{2(1 + R_p)} \quad (6)$$

$L(\omega)$ is roughly the same as the c-axis loss function $\text{Im}(-1/\epsilon_c)$ apart from a weakly frequency dependent phase-shift $\phi = \pi/2 - \text{Arg}(n_{ab})$. The second equality in Eq.6 can be used to calculate $L(\omega)$ from the grazing incidence reflectivity data. Although this requires an estimate of $|n_{ab}|$, as $|n_{ab}|$ has a smooth frequency-dependence, the multiplication with this factor does not influence the position and line shape of the c-axis longitudinal modes.

The p-polarized reflectivity was measured at an angle of incidence of $\theta = 80^\circ$. To increase the probing area, we mounted a mosaic of four crystals which was fixed on top of a cone in order to reject stray light. Absolute reflectivities were obtained by referencing the intensity reflected from the samples to the reflectivity after Au-coating the samples *in situ*. In Fig. 2 we present the grazing incidence reflectivity of the $\text{Ti}_2\text{Ba}_2\text{CuO}_{6+\delta}$ crystal. R_p is characterized by a strong increase with decreasing temperature, which is caused by the temperature dependence

of the in-plane optical conductivity. For $T = 6$ K we observe deep and narrow minima [12] at 157, 429, 631 cm^{-1} , which lie close to the out-of plane frequencies (143, 451 and 648 cm^{-1}) obtained from lattice dynamical calculations [13]. Surprisingly an LO apex-oxygen bending mode predicted at 348 cm^{-1} with a relatively large oscillator strength is absent in our data, similar to what was observed for $\text{Ti}_2\text{Ba}_2\text{Ca}_2\text{Cu}_3\text{O}_{10}$ [14]. From Eq.3 we see, that the half-width of the LO-phonons in the loss function ($\text{Im}1/\epsilon_c$) is given by $1/\tau + 4\pi\sigma_e\epsilon_\infty^{-1}S/(\epsilon_\infty + S)$, where τ is the intrinsic phonon life-time, S the oscillator strength, and σ_e the electronic optical conductivity. Hence the width of these peaks can be used to estimate σ_e . After correcting for peak-asymmetries of the pseudo-loss function introduced through the phase-shift ϕ , we obtained that $\sigma_e = 0.7 \pm 0.3$ S/cm near 500 cm^{-1} , *i.e.* below the DC conductivity at 100 K (2 S/cm). Two strongly damped modes at 86 and 538 cm^{-1} are close to the calculated in-plane mode frequencies (84 and 560 cm^{-1}). Having established these best-fit parameters for the optical phonons we were able to determine the electronic contribution of the in-plane optical conductivity by fitting the experimental data over a wide frequency range (50 to 6000 cm^{-1}) to Eq.4. Our estimated in-plane optical conductivity is in excellent agreement with recent results by Puchkov *et al.* [15].

Although in the normal state the free carrier c-axis plasmon is known to be overdamped in the cuprates, in the superconducting state we expect to observe a plasma minimum in R_p at the screened plasma resonance $\omega_{ps}/\sqrt{\epsilon_S}$ [16] where ϵ_S is the background dielectric function (see Eq.3). To demonstrate the reliability of the grazing incidence method we display in the lower part of Fig. 3 R_p measured on the ab-plane of a $\text{La}_{2-x}\text{Sr}_x\text{CuO}_4$ single crystal. Below T_c a minimum occurs, which sharpens and shifts to 50 cm^{-1} upon reducing temperature, consistent with the temperature dependence of ω_J found from normal incidence reflectivity measurements [17] on the ac-plane of this crystal. Such a structure is not present in the far-infrared or mid-infrared reflectivity spectra for the $\text{Ti}_2\text{Ba}_2\text{CuO}_6$ single crystal (Fig. 2) in the measured frequency range. Since at low frequencies the signal/noise ratio is limited by the small size of the crystals, we also measured R_p of thin films of $\text{Ti}_2\text{Ba}_2\text{CuO}_6$ in the frequency range from 20 to 8000 cm^{-1} . We observed the same overall behaviour and optical phonon spectrum as for the single crystal except for an additional optical phonon of the SrTiO_3 -substrate at 170 cm^{-1} . The reflectivity is shown on an expanded scale in the upper panel of Fig. 3. Even with the strongly improved signal/noise ratio no clear evidence for a Josephson plasmon is present in these data, except perhaps for a rather broad and shallow minimum at 40 cm^{-1} .

To enable a direct comparison to theory, we display in Fig. 4a the c-axis pseudo loss function for $\text{Ti}_2\text{Ba}_2\text{CuO}_6$, both in the normal and in the superconducting state, cal-

culated from the reflectivity spectra (Fig. 2) using Eq.6, while adopting a smoothly frequency dependent ab -plane dielectric function ϵ_{ab} fitted to R_p over a wide frequency range upto 8000 cm^{-1} . In Figs. 4b-4d we display model calculations of the pseudo-loss function based on the two scenario's (BCS and ILT) outlined in the introduction. We used the optical phonon parameters discussed above [12]. The phase shift ϕ was calculated from the in-plane dielectric function mentioned above. In Figs. 4c and 4d the superconducting response was calculated with a Josephson plasma frequency calculated from the BCS expression (Eq.2). In Fig. 4c it was assumed that there is no residual c-axis optical conductivity at the position of the Josephson plasma resonance (50 cm^{-1}). In 4d a small residual conductivity of 3 S/cm was added near the resonance. Such a residual conductivity is expected in the case of d-wave pairing in the presence of impurity scattering. We notice that the occurrence of the Josephson plasmon at 50 cm^{-1} has no noticeable effect on the position of the three longitudinal optical phonons at 155 , 430 and 630 cm^{-1} . The solid curve in Fig. 4b represents a simulation of the superconducting state adopting $\omega_J = 1500\text{ cm}^{-1}$ implied by the ILT model (Eq.1), while keeping all other c-axis parameters unaltered. The three peaks are now of mixed phonon-plasmon character. The large value of the Josephson plasma frequency results in a considerable shift of the two peaks at 430 and 630 cm^{-1} towards lower frequencies, and a strong suppression of intensity of the 155 cm^{-1} mode. The peak at 700 cm^{-1} is essentially a screened superfluid plasmon.

Experimentally no Josephson plasmon is observable in Fig. 2, 4a or for the film in Fig. 3 except perhaps for a rather broad feature around 40 cm^{-1} in Fig. 3. Taken together with the fact that there is no observable shift of the LO phonons at 146 , 379 , and 594 cm^{-1} as the temperature is reduced from 300 K to 6 K , an upper limit can be set for the screened plasma resonance of 40 cm^{-1} . Using the fitted phonon-parameters and ϵ_∞ for $\vec{E} \parallel \vec{c}$ [12], this implies that the unscreened Josephson plasma frequency satisfies $\omega_J < 100\text{ cm}^{-1}$, or equivalently the c-axis penetration depth satisfies $\lambda_c > 15\mu\text{m}$ for $T \rightarrow 0$. For $\text{La}_{2-x}\text{Sr}_x\text{CuO}_4$ and $\text{Tl}_2\text{Ba}_2\text{CuO}_6$ the fraction of the condensation energy contributed by the ILT mechanism $\eta = (\omega_J^{\text{exp}}/\omega_J^{\text{ILT}})^2 \approx 0.2$ and $\eta < 0.005$ respectively. $\text{Tl}_2\text{Ba}_2\text{CuO}_6$ differs from $\text{La}_{2-x}\text{Sr}_x\text{CuO}_4$ in other respects: The very low normal state c-axis conductivity ($< 2\text{ S/cm}$ at 100 K) combined with a linear rise as a function of temperature has been noticed before and is confirmed both from our DC measurements and from the dynamical conductivity around 500 cm^{-1} obtained from our analyzes of the line shape of the prominent longitudinal optical phonons. These observations, and the very low c-axis Josephson plasma frequency definitely pose a challenge both to 'conventional' mechanisms and to the implementation of the ILT model as it was described in Ref. [1]. To comply with these facts within the context

of an ILT mechanism one may postulate [18] the existence of small electron pockets in the TlO layers, which are also two-dimensional and cross the main CuO band only at a few points in 2D k -space. The matrix element which would uncross these bands is then restricted in 2D k -space, which leads to a reduced value of ω_J^2 , while T_c depends mainly on those parts of Fermi surface where the crossing occurs. Within this scenario large portions of the Fermi surface should exist where $|\Delta| \ll |\Delta_{\text{max}}|$, which can be tested experimentally.

We measured the c-axis infrared properties of thin plate-like $\text{Tl}_2\text{Ba}_2\text{CuO}_6$ single crystals and thin films and the ab-face of $\text{La}_{2-x}\text{Sr}_x\text{CuO}_4$ using grazing incidence infrared spectroscopy. The screened plasma resonance of $\text{Tl}_2\text{Ba}_2\text{CuO}_6$ was found to be below 40 cm^{-1} , corresponding to an unscreened c-axis Josephson plasma frequency of 100 cm^{-1} and a lower limit of the c-axis penetration depth of $15\mu\text{m}$. These experimental results, together with the low value of the conductivity along the c-direction, pose a challenge both to conventional theories and the inter layer tunneling mechanism.

Acknowledgements One of us (D.v.d.M) gratefully acknowledges numerous fruitful discussions with P.W. Anderson and A.J. Leggett at various stages of this project. This investigation was supported by the Netherlands Foundation for Fundamental Research on Matter (FOM) with financial aid from the Nederlandse Organisatie voor Wetenschappelijk Onderzoek (NWO) and by the EEC (Human Capital and Mobility). The work performed at SUNY/Buffalo was supported by NY-SERDA, ORNL, ANL, ONR, and NSF.

-
- [1] S. Chakravarty and P.W. Anderson, Phys. Rev. Lett. **72**, 3859 (1994).
 - [2] P.W. Anderson, Science **268**, 1154 (1995).
 - [3] D. van der Marel, *10th Anniversary HTS Workshop on Physics, Materials and Applications*, Houston, March 1996, in press.
 - [4] A.J. Leggett, submitted to Science (1996).
 - [5] J. Loram, private communication.
 - [6] M. Tinkham, *Introduction to Superconductivity* (Mc Graw-Hill, New York, 1996)
 - [7] N. N. Kolesnikov *et al.*, Physica C **242** 385 (1995).
 - [8] H.M. Duan *et al.*, Physica C **185**, 1283 (1990); T. Manako *et al.*, Physica C **185**, 1327 (1990).
 - [9] C. A. Wang *et al.*, Physica C **262**, 98 (1996).
 - [10] H.S. Somal *et al.*, Phys. Rev. Lett. **76** 29 february, (1996).
 - [11] O.K.C. Tsui, N.P. Ong, and J.B. Peterson, Phys. Rev. Lett. **76**, 819 (1996).
 - [12] Using Eq.3 the fit parameters of the phonons are $\epsilon_\infty = 4.0$ and $\{\omega_{Tj}(\text{cm}^{-1}), S_j, 1/\tau_j(\text{cm}^{-1})\} = \{146, 0.30, 1\}, \{379, 0.93, 8\}, \{594, 0.31, 8\}$ ($j = 1..3$).
 - [13] A.D. Kulkarni *et al.*, Phys. Rev. B **41**, 6409 (1990).

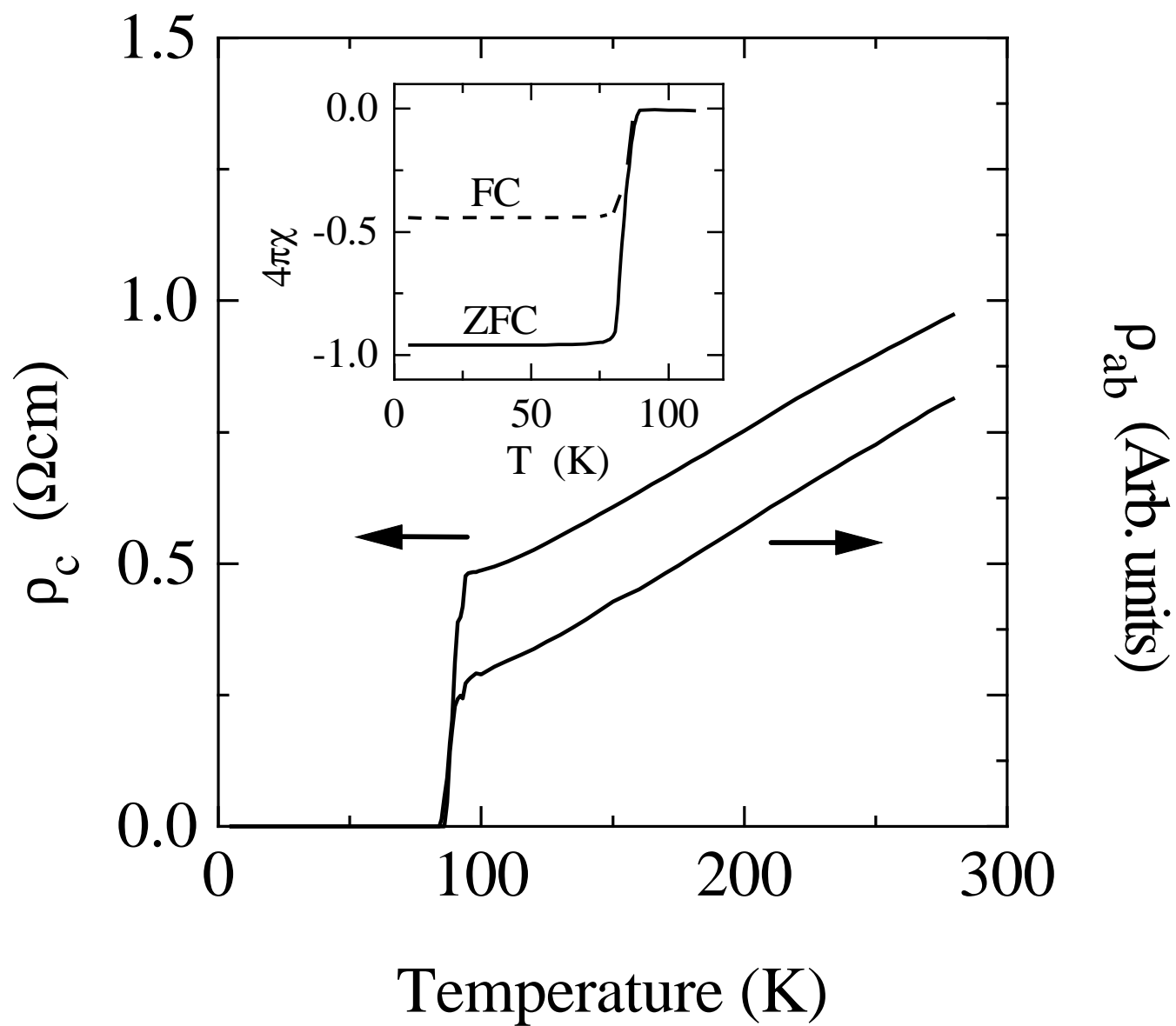
- [14] Jae Kim *et al*, Phys. Rev. B, 49 (1994) 13065-13069
- [15] A.V. Puchkov *et al*, Phys. Rev. B **51**, 3312 (1990).
- [16] K. Tamasaku, Y. Nakamura, and S. Uchida, Phys. Rev. Lett. **69** (1992) 1455
- [17] J. H. Kim, A. Wittlin, D. van der Marel *et al.*, Physica C **247**, 297 (1995).
- [18] P.W. Anderson, private communication.

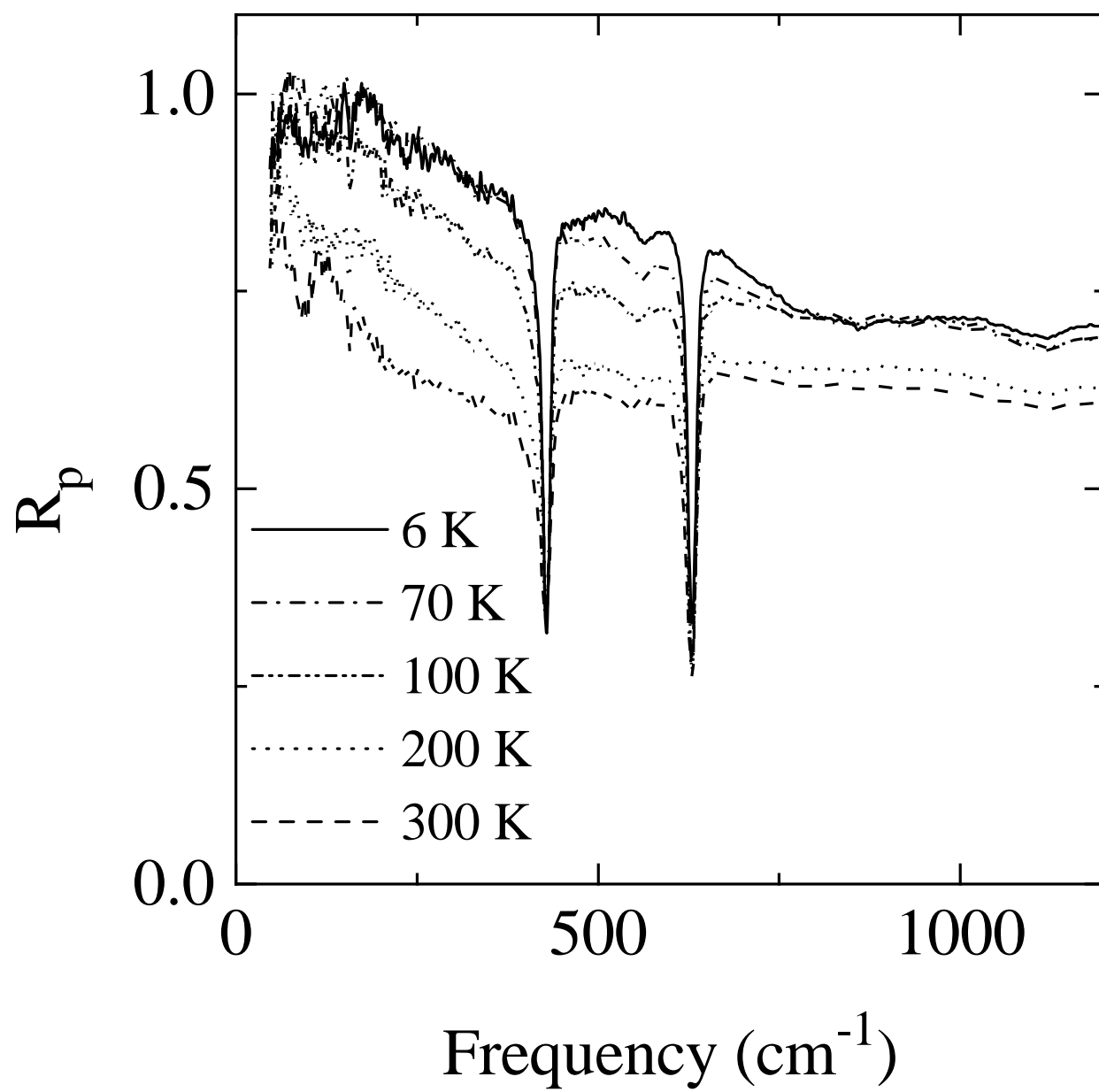
FIG. 1. dc resistivity and dc susceptibility measured with $H \parallel ab$ (10 Oe) of a $Tl_2Ba_2CuO_6$ single crystal.

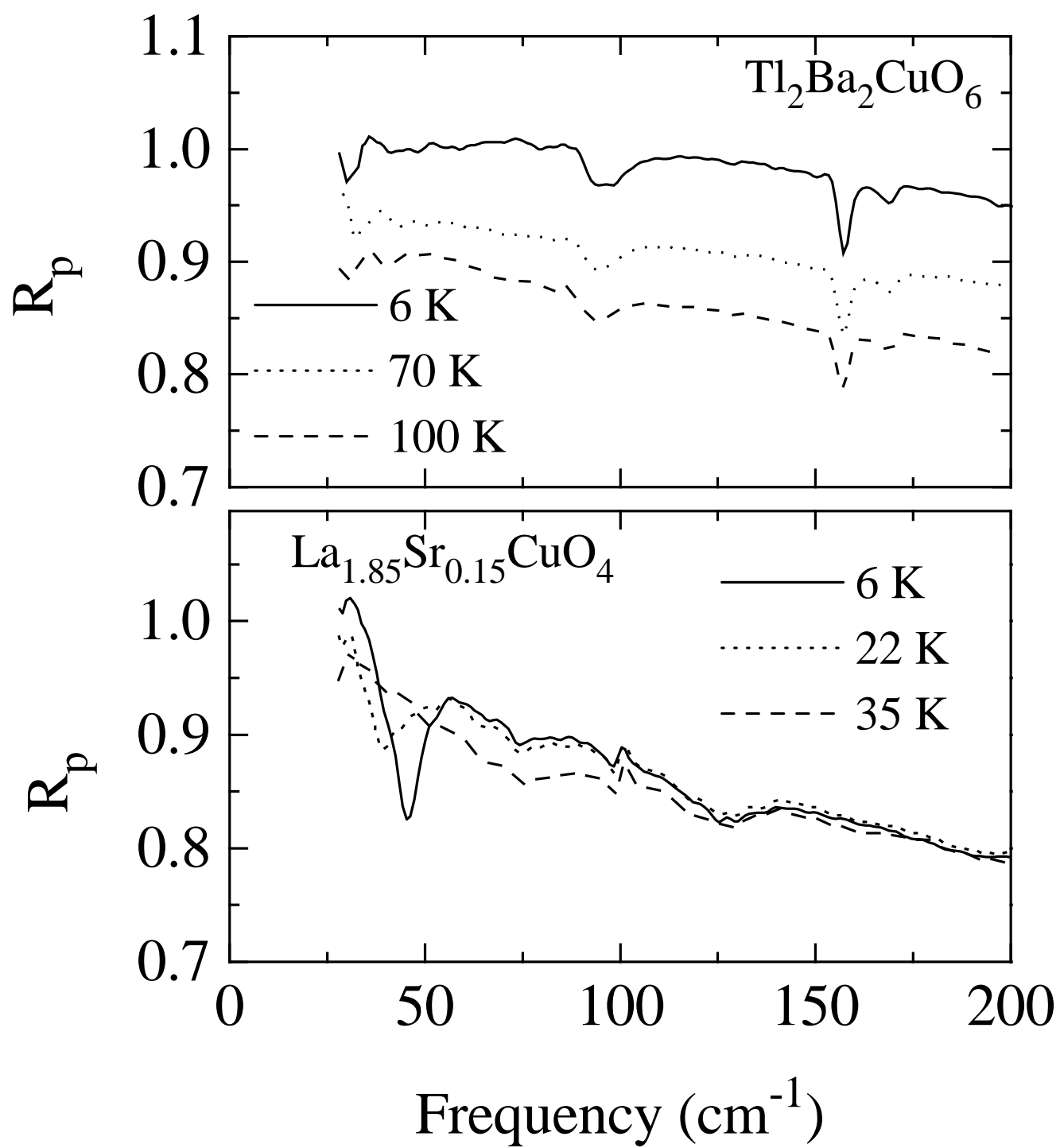
FIG. 2. Reflectivity R_p of a $Tl_2Ba_2CuO_6$ single crystal measured with p-polarized light incident on the ab-surface at an angle of 80° .

FIG. 3. Reflectivity R_p of a $Tl_2Ba_2CuO_6$ thin film (upper panel) and of a $La_{1.85}Sr_{0.15}CuO_4$ single crystal measured with p-polarized light incident on the ab-surface at an angle of 80° .

FIG. 4. Pseudo loss function $L(\omega)$ of $Tl_2Ba_2CuO_6$: (a) experimental data at 100 K (dashed curve) and 6 K (solid), (b) simulation for the normal state (dashed) and for the superconducting state (solid) adopting the ILT value for ω_J of 1500 cm^{-1} , (c) simulation of the superconducting state adopting the BCS value for ω_J of 200 cm^{-1} , (d) *idem.* with a residual Drude conductivity of 3 S/cm added close to the plasma resonance. In (b),(c) and (d) σ_e was set to 0.5 S/cm near the dominant phonon frequencies.







Pseudo Loss Function

